Proc. Natl. Acad. Sci. USA
Vol. 80, pp. 1241–1245, March 1983
Biochemistry

Rates of enzyme-catalyzed exchange determined by two-dimensional NMR: A study of glucose 6-phosphate anomerization and isomerization

(phosphoglucose isomerase/steady state)

R. S. BALABAN* AND J. A. FERRETTI†

*Laboratory of Kidney and Electrolyte Metabolism, National Heart, Lung, and Blood Institute, Building 10, Room 6N323; and †Division of Computer Research and Technology, National Institutes of Health, Bethesda, Maryland 20205

Communicated by F. A. Bovey, December 1, 1982

ABSTRACT **The application of two-dimensional (2D) Fourier-transform NMR to the determination of rate constants of complex enzyme-catalyzed reactions in the steady state is described. The yeast phosphoglucose isomerase (EC 5.3.1.9)-catalyzed anomerization of glucose 6-phosphate (Glc-6-*P*) as well as its isomerization to fructose 6-phosphate (Fru-6-*P*) was chosen as an example. The 2D technique permitted the simultaneous monitoring of the time course of the anomerization and isomerization steps, from which the various reaction rates were determined. The results obtained in the steady state demonstrate the usefulness of the 2D technique by confirming that the anomerization of Glc-6-*P* is enzyme catalyzed and that the isomerization of the α anomer of Glc-6-*P* to Fru-6-*P* is at least 10 times faster than the isomerization of the β anomer of Glc-6-*P*. These results are compared with reaction rates obtained by rapid-quench methods and the mechanistic implications are discussed. Extrapolation of these results suggests that the 2D Fourier-transform NMR method should be applicable in intact biological tissues.**

Knowledge of the rate constants of enzyme-catalyzed reactions is necessary for a complete understanding of the mechanism and control of enzymatic processes both *in vivo* and *in vitro*. Several techniques are presently available to determine these rates; these include stop-flow, temperature-jump, radioisotope exchange, and various types of nuclear magnetic resonance (NMR) spectroscopic techniques (1). Of these various techniques only NMR is sufficiently noninvasive to be used to study enzymatic processes *in vivo* and thus has great potential in unraveling the rates and regulation of enzyme-catalyzed reactions in intact cells.

Rate constant measurements by NMR can be carried out by linewidth analysis (2, 3) and saturation and inversion transfer of magnetization (4, 5), as well as by selective saturation or inversion recovery relaxation experiments (2, 6). The linewidth analysis method is applicable when the exchange rate is of the same order of magnitude as the chemical shift differences (Hz) between the exchanging species. However, this technique, in addition to being limited to a narrow range of rate constants, cannot in practice be applied to complex reaction pathways such as those found in enzyme-catalyzed processes. Saturation and inversion transfer have generally been the methods of choice for measuring moderately slow enzymatic rate constants, because one can follow the direct transfer of magnetization between exchanging species. However, magnetization transfer requires the application of a second irradiating rf field, which can present difficulties on commercial spectrometers and which limits selectivity in a crowded or complex spectrum. These experiments usually rely on the detection of small differences in peak areas, which limits precision.

A recently introduced two-dimensional Fourier-transform NMR (2D FTNMR) technique (called 2D NOESY, for nuclear Overhauser enhancement spectroscopy) is capable of mapping out complex reaction paths and shows great potential for yielding rate constants in the steady state with a high degree of precision. The use of 2D FTNMR to determine chemical reaction rates has been extensively discussed by Ernst and co-workers (7–9). This technique, as well as other magnetization transfer experiments, takes advantage of a transient frequency label imposed on an individual nucleus in an exchanging system to noninvasively monitor the reaction pathways. An important advantage of the 2D method is that separate peaks appear in the 2D matrix that represent molecules that have undergone chemical exchange in a prescribed time interval. Thus, in the 2D experiment all exchange pathways are observed simultaneously in a single study, which can amount to a significant savings in time. Also, difficulties with using a selective pulse in a crowded region of a spectrum are avoided. Such a situation usually exists in the case of a substrate and its enzyme complex, for which the chemical shift differences between the two nuclei can be small. In addition, the 2D method allows a straightforward analysis and the initial rate approximation yields rate constants without any knowledge of the spin lattice relaxation times, T_1.

Phosphoglucose isomerase is an enzyme that catalyzes the isomerization of glucose 6-phosphate (Glc-6-*P*) to fructose 6-phosphate (Fru-6-*P*). The rates associated with this reaction have been extensively studied by rapid-quench techniques, and it has been shown that the enzyme has a marked preference for the α forms of Glc-6-*P* and Fru-6-*P* as substrates. Separate peaks are observed in the ^{31}P NMR spectra for Glc-6-*P* and Fru-6-*P*. Furthermore, these spectra are not complicated by homonuclear scalar spin coupling. Thus, this simple system is advantageous for investigating the feasibility of using 2D FTNMR to measure enzyme-catalyzed rates of reaction and to compare the results with rapid-quench data on a well-studied system.

METHODS AND MATERIALS

Methods. The 2D exchange experiment consists of the following three 90° pulses, shown in Fig. 1. The first pulse, followed by an evolution period, t_1, is used to frequency label the magnetization. The second pulse rotates the y component of the magnetization onto the z axis, thereby interrupting the time development of the nuclear precession. In addition, a homogeneity-spoiling pulse is applied immediately after the second pulse

The publication costs of this article were defrayed in part by page charge payment. This article must therefore be hereby marked "*advertisement*" in accordance with 18 U. S. C. §1734 solely to indicate this fact.

Abbreviations: 2D, two-dimensional; FTNMR, Fourier-transform NMR; NOESY, nuclear Overhauser enhancement spectroscopy; Glc-6-*P*, glucose 6-phosphate; Fru-6-*P*, fructose 6-phosphate.

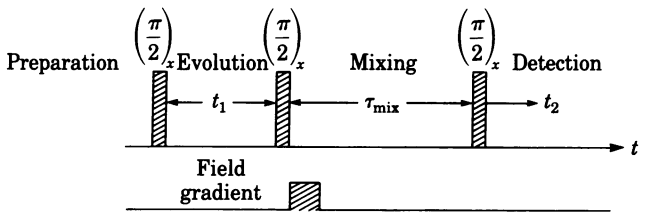

FIG. 1. Basic three-pulse sequence for 2D NOESY experiment.

to destroy any residual magnetization in the xy plane. Although the homogeneity-spoiling pulse can destroy the field-frequency lock condition, our experience is that careful preadjustment of the field to minimize "pulling" by the lock system permits us to destroy the homogeneity for at least 30 msec with no adverse effects. The third pulse then restarts the time development of the nuclear magnetization, and this signal is recorded in the computer. Processes such as cross-relaxation or chemical exchange can interconvert the frequency-labeled nuclei during the mixing interval, τ_{mix}, between the second and third pulses. After systematic variation of t_1, the resulting matrix of free induction decays, $g(t_1,t_2)$, is then double Fourier transformed to produce the desired 2D spectrum with frequency axes F_1 and F_2. Molecules that did not undergo chemical conversion during τ_{mix} will show the same resonance frequencies along the substrate axis, F_1, and along the product axis, F_2, because their precession frequencies were the same during both t_1 and t_2. These peaks are found along a diagonal in a 2D (F_1,F_2) plot. Molecules that underwent chemical conversion during τ_{mix} will have resonance frequencies of the substrate along F_1 and resonance frequencies of the product along F_2. These peaks are termed cross peaks because they are found at the crossing of the perpendiculars drawn at the appropriate resonance frequencies along F_1 and F_2. The 2D spectrum qualitatively defines the complete exchange pattern occurring in the sample for the molecular system under study. However, to determine the various rate constants, it is necessary to record a series of 2D spectra by varying τ_{mix}. Evaluation of the dependence of the cross peak volumes on τ_{mix} then permits one to compute the rate constants for the relevant exchange processes.

Materials. Phosphoglucose isomerase (glucosephosphate isomerase; D-glucose-6-phosphate ketol-isomerase, EC 5.3.1.9) from yeast was obtained from Sigma (lot 45c-8565). The enzyme suspension was dialyzed overnight (1:1,000, vol/vol) in 120 mM potassium Hepes/2 mM EDTA, pH 7.2 at 6°C. The resulting suspension was filtered through Whatman no. 1 filter paper and assayed for activity. The activity of phosphoglucose isomerase (10) was checked at 25°C in a solution containing 120 mM potassium Hepes at pH 8.0, 5 mM Fru-6-*P*, 0.2 mM NADP, and glucose-6-phosphate dehydrogenase at 0.2 unit/ml. D-Glc-6-*P* was obtained from Sigma (lot no. 88C-3880) and titrated with NaOH to pH 7.4. All experiments were performed in the presence of 10% (vol/vol) ^2H_2O to provide a field-frequency lock for the spectrometer.

All experiments were performed on a Nicolet NT360 spectrometer detecting ^{31}P at 146.15 MHz. The carrier frequency was set at one side of the spectrum and detection was done with a single-phase detector (i.e., quadrature phase detection off).

RESULTS

Fig. 2 shows the one-dimensional ^{31}P NMR spectrum of an equilibrium mixture of Glc-6-*P* and Fru-6-*P* in the presence of yeast phosphoglucose isomerase. The α and β anomers of Glc-6-*P* are resolved, indicating that the anomerization in the pres-

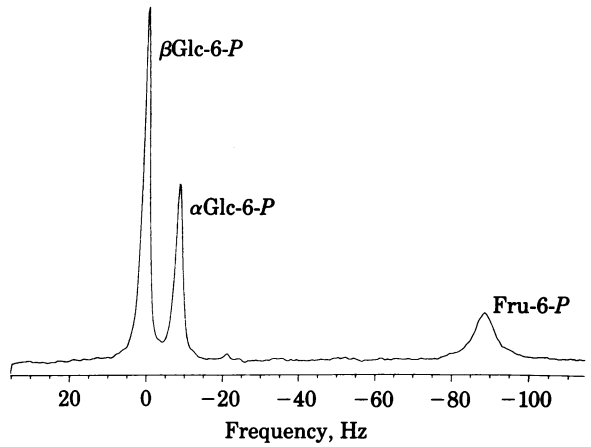

FIG. 2. ^{31}P NMR spectrum of an equilibrium mixture of Glc-6-*P* and Fru-6-*P*. The solution was prepared by adding 6,000 units of yeast phosphoglucose isomerase to 68 mM Glc-6-*P* containing 125 mM KCl, 25 mM potassium Hepes, 0.5 mM EDTA, and 10% ^2H_2O at pH 7.4. The spectrum represents the average of 12 free induction decays after a 90° pulse with 17-sec delays between each acquisition.

ence of enzyme occurs more slowly than the chemical shift difference between the Glc-6-*P* anomers. The appearance of Fru-6-*P* as a single broad peak suggests that its anomerization rate is somewhat greater than the chemical shift difference of the Fru-6-*P* anomers. Thus, the data obtained in the 2D experiment will provide rate information only on the average of both anomers of Fru-6-*P* and not on the formation of the individual α and β anomers. Integration of the spectrum in Fig. 2 yields 0.53, 0.27, and 0.20 as the equilibrium mol fractions of αGlc-6-*P*, βGlc-6-*P*, and α- and βFru-6-*P*, respectively. A ^{31}P 2D NOESY stack plot and contour plot of the same mixture are shown in Fig. 3 *A* and *B*, respectively. The general features of the expected 2D spectrum are outlined in Fig. 4. The αGlc-6-*P*, βGlc-6-*P*, and Fru-6-*P* that did not undergo chemical conversion occur at the same values along both F_1 and F_2 and are observed on the (F_1,F_2) diagonal in a 2D plot. The nuclei that did undergo chemical conversion have values along F_1 of the substrate and values along F_2 of the product. Cross peaks in Fig. 3 can be seen for both the anomerization and isomerization reactions of phosphoglucose isomerase. The noise along the F_2 frequency axis has been discussed previously (7–9) and, if excessive, can sometimes be reoriented by shifting the carrier frequency to the other side of the spectrum in order to observe obscured cross peaks. In the case of the anomerization reaction, the αGlc-6-*P* that is formed from βGlc-6-*P* during the 1-sec mixing time of this experiment is found at the (F_1,F_2) coordinates that correspond to the frequency of the βGlc-6-*P* diagonal peak along F_1 and the frequency of the αGlc-6-*P* diagonal peak along F_2. For the isomerization reaction, the αGlc-6-*P* that became Fru-6-*P* is found at the (F_1,F_2) coordinates that correspond to the frequency of the αGlc-6-*P* along F_1 and the frequency of the Fru-6-*P* diagonal peak along F_2.

As an indication of the reliability of the 2D method in determining rate constants, we examined the well-characterized nonenzymatic anomerization of Glc-6-*P* at 37°C. This reaction can be treated as a first-order exchange between αGlc-6-*P* and βGlc-6-*P*:

$$\alpha\text{Glc-6-}P \underset{k_{\beta\alpha}}{\overset{k_{\alpha\beta}}{\rightleftarrows}} \beta\text{Glc-6-}P$$

The expressions for the τ_{mix} dependence of the diagonal peak

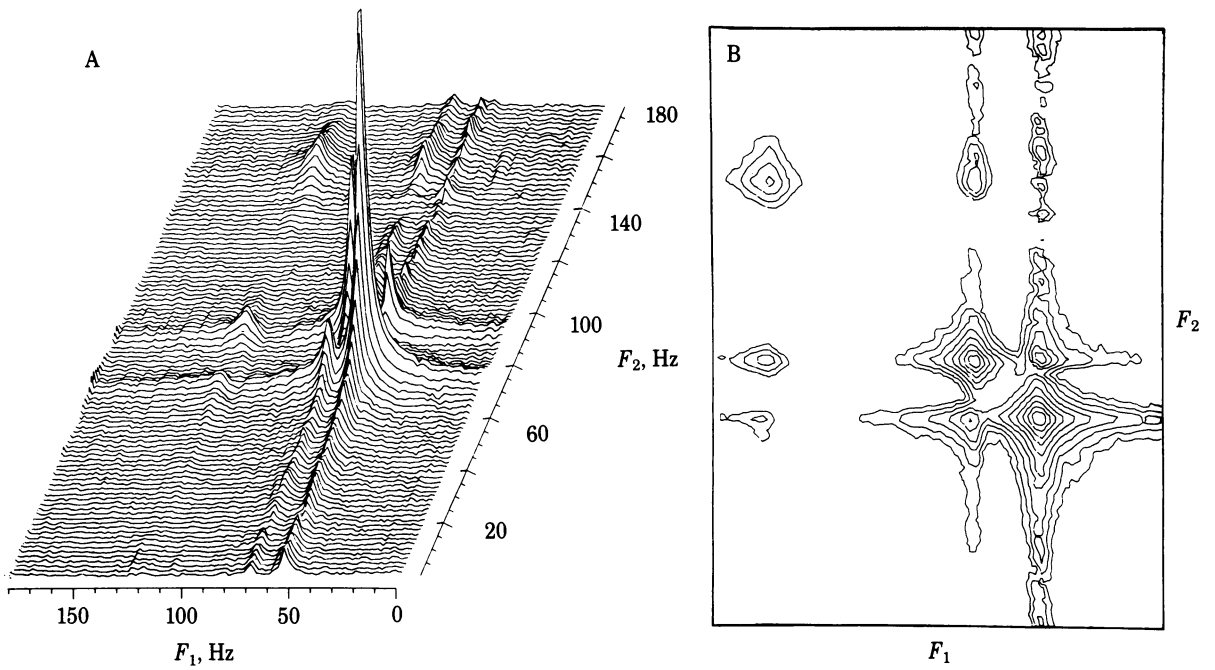

FIG. 3. 2D plots of a ^{31}P 2D NOESY experiment on the mixture described for Fig. 2. The τ_{mix} was 1 sec. For details of the experiment see text. (*A*) Stack plot of data; (*B*) Contour plot of same data.

volumes ($I_{\alpha\alpha}$ and $I_{\beta\beta}$) for the anomerization reaction are:

$$I_{\alpha\alpha} = {}^1/_2 X_\alpha (1 + e^{-(k_{\alpha\beta} + k_{\beta\alpha})\tau_{mix}}) e^{-\tau_{mix}/T_1} \quad [1]$$

$$I_{\beta\beta} = {}^1/_2 X_\beta (1 + e^{-(k_{\alpha\beta} + k_{\beta\alpha})\tau_{mix}}) e^{-\tau_{mix}/T_1}. \quad [2]$$

The τ_{mix} dependence of the cross peaks is expressed as:

$$I_{\alpha\beta} = I_{\beta\alpha} = X_\alpha X_\beta (1 - e^{-(k_{\alpha\beta} + k_{\beta\alpha})\tau_{mix}}) e^{-\tau_{mix}/T_1}. \quad [3]$$

The expressions in Eqs. 1–3 contain the equilibrium mol fractions X_α and X_β, the two rate constants $k_{\alpha\beta}$ and $k_{\beta\alpha}$, and the spin lattice relaxation time T_1. The expressions are presented only for equal values for the relaxation times of αGlc-6-*P* and βGlc-6-*P*, but they could be modified to include unequal T_1 values. In this simple two-site exchange, one can determine the rate constants by fitting the entire curve of cross-peak volumes versus τ_{mix}. An alternative method, which is essential for the study of more complex systems, involves determining the initial rate of product formation. An expression for the initial slope from Eq. 3 may be written as:

$$\left(\frac{dI_{\alpha\beta}}{dt}\right)_{\tau_{mix}\to 0} = X_\alpha k_{\alpha\beta}. \quad [4]$$

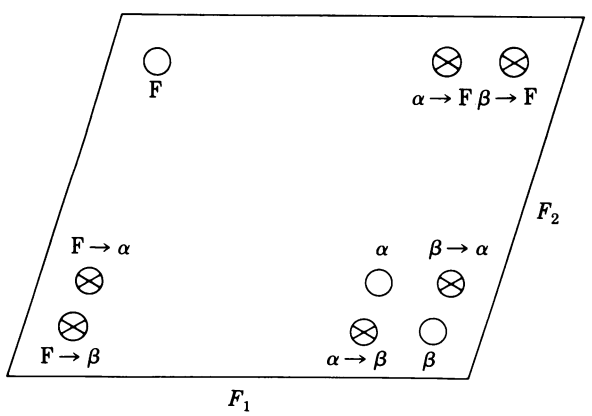

FIG. 4. General features of the 2D NOESY contour plot. Peaks: F, Fru-6-*P*; α, αGlc-6-*P*; β, βGlc-6-*P*.

Two points to note from Eq. 4 are that the unidirectional rate constant is obtained from the initial time behavior of a single cross peak and that the initial slope is independent of T_1. The time course of the anomerization at 37°C is shown in Fig. 5. Fig. 5*A* illustrates the cross section through the 2D plot for a fixed frequency value along F_2 chosen to be at the peak. Fig. 5*B* is a graph of the volumes of the cross peaks versus τ_{mix}. A summary of the rate constants, determined by 2D FTNMR, both by using the initial slope method and by fitting the entire curve, and data from optical rotation studies (11) is shown in Table 1. Note that both the initial slope method and the complete curve analysis yield rate constants that are in agreement with the optical rotation data.

Systematic variation of τ_{mix} in the study of the enzyme-catalyzed reaction yields the curves shown in Fig. 6 for the isomerization of Fru-6-*P* to αGlc-6-*P* and to βGlc-6-*P*. We note that the isomerization to βGlc-6-*P* occurs only after an induction period. Also, because of the proximity of the resonances of the αGlc-6-*P* and βGlc-6-*P*, observation of the anomerization reaction by the usual one-dimensional techniques would be quite difficult. The simple kinetic scheme outlined in Fig. 7 was used to derive the initial slope expressions for the various rates. By using these expressions the rates listed in Table 2 were obtained. The rates of anomerization in the presence and absence of enzyme demonstrate that this reaction is indeed enzyme catalyzed. In addition, the zero initial slope observed for the formation of Fru-6-*P* from βGlc-6-*P* demonstrates that βGlc-6-*P* is not directly formed from Fru-6-*P*. This suggests that the βGlc-6-*P* is initially converted to αGlc-6-*P* and subsequently is isomerized to Fru-6-*P*. These data are consistent with the conclusion that direct isomerization of βGlc-6-*P* to Fru-6-*P*, if it occurs at all, is at a rate of less than 0.04 sec^{-1} in the steady state.

DISCUSSION

The results on the phosphoglucose isomerase-mediated isomerization and anomerization of Glc-6-*P* and Fru-6-*P* show that 2D FTNMR can simultaneously monitor the various pathways in a complex reversibly exchanging system under steady-state conditions. Furthermore, the unidirectional rate data are ob-

*Correction - Proc. Nath Acad Sci USA, 80 (1983)

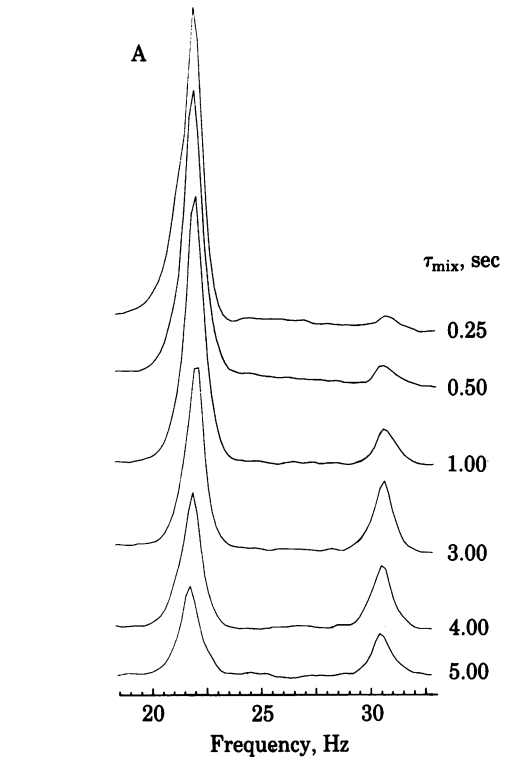

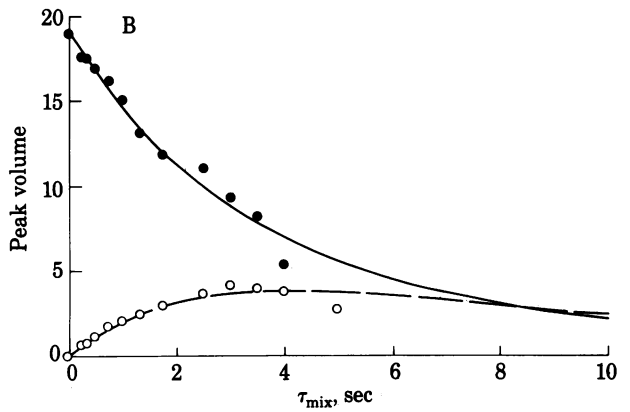

FIG. 5. Anomerization of Glc-6-*P* at 37°C in the absence of enzyme. (*A*) Cross section through the 2D plot for the diagonal peak of αGlc-6-*P* as a function of τ_{mix}. (*B*) Volume of the cross peaks (○) and diagonal peaks (●) as a function of τ_{mix}.

tained noninvasively. The rates are obtained from the data without specific knowledge of the spin lattice relaxation times, T_1, of the various species involved in the exchange process and with little interference from enzyme–substrate complexes. These latter features, coupled with the separate appearance in the 2D matrix of peaks corresponding to species that have reacted during the mixing period, τ_{mix}, allow the estimation of the various rate constants in a fixed time period with improved precision over the usual magnetization transfer experiments.

As with all magnetization transfer experiments, the technique can monitor reactions with rate constants only within specific limits. The upper limit is the relevant chemical shift differences between the exchanging species. If the reaction is too fast, separate resonances for the exchanging species will not be observed. The lower limit is governed by the ability to obtain cross-peak build-up before complete relaxation occurs. Thus, the rate constant must be at least similar to the relaxation rate in order to measure appreciable cross-peak volumes. This means that the product formation must occur faster than the decrease in signal volume due to spin lattice relaxation. For ^{31}P NMR *in vivo* and *in vitro*, this corresponds to rates of the order of 1 sec^{-1}. However, it should be emphasized that knowledge of T_1 is not necessary for the determination of the rate constants as long as the initial rates can be determined. Nevertheless, some systems

Table 1. Rate constants (sec^{-1}) at 37°C for Glc-6-*P* anomerization

	2D FTNMR		
k	Initial rate	Curve fit	Mutarotation*
$k_{\alpha\beta}$	0.43 (X_α = 0.34)	0.43	0.44 (X_α = 0.38)
$k_{\beta\alpha}$	0.22 (X_β = 0.66)	0.22	0.27 (X_β = 0.62)

*Ref. 11.

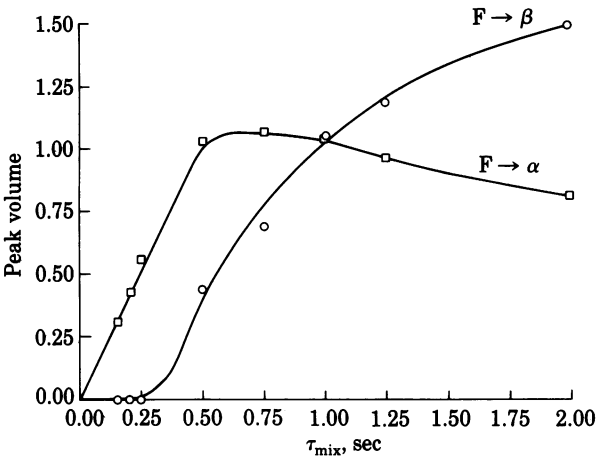

FIG. 6. Volume of the Fru-6-*P* to α- and βGlc-6-*P* cross peaks as a function of τ_{mix}. The conditions were identical to those for Fig. 2. Symbols for sugar phosphates are as in Fig. 4.

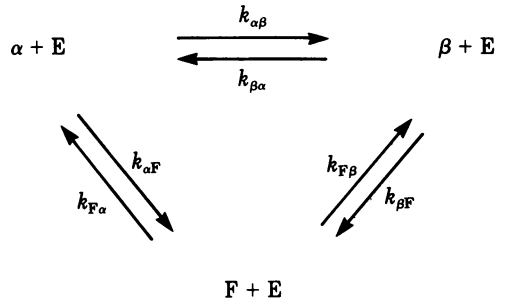

$$\left(\frac{dI_{\alpha\beta}(\tau_{mix})}{d\tau_{mix}}\right)_{\tau_{mix}\to 0} = X_\alpha k_{\alpha\beta}E = X_\alpha V^{\alpha\beta}_{max}$$

$$\left(\frac{dI_{F\alpha}(\tau_{mix})}{d\tau_{mix}}\right)_{\tau_{mix}\to 0} = X_F k_{F\alpha}E = X_F V^{F\alpha}_{max}$$

$$\left(\frac{dI_{F\beta}(\tau_{mix})}{d\tau_{mix}}\right)_{\tau_{mix}\to 0} = X_F k_{F\beta}E = X_F V^{F\beta}_{max}$$

FIG. 7. Schematic model of the phosphoglucose isomerase reaction and initial rate equations. E, enzyme; *I*, peak volume; sugar phosphates as in Fig. 4.

Table 2. Rates of reactions catalyzed by phosphoglucose isomerase

Reaction	Rate, sec^{-1} (25°C)	
	Enzyme	No enzyme
αGlc-6-*P* → βGlc-6-*P*	0.29	0.06
βGlc-6-*P* → αGlc-6-*P*	0.15	0.036
Fru-6-*P* → αGlc-6-*P*	3.4	
αGlc-6-*P* → Fru-6-*P*	2.5	
Fru-6-*P* → βGlc-6-*P*	<0.04	
βGlc-6-*P* → Fru-6-*P*	<0.04	

with very short relaxation times may not be amenable to investigation by magnetization transfer.

The 2D FTNMR experiment generally requires the acquisition of a large amount of data and thus a corresponding long period of time for data collection. For the *in vitro* study of Glc-6-*P*, it was possible to work at high substrate and enzyme concentrations so that data for one value of τ_{mix} were obtained in 40 min and processing time took an additional 20 min. Preliminary *in vivo* studies using a specially constructed probe and a surface coil design have been carried out on an anesthetized rat (unpublished data). Here the creatine kinase-catalyzed exchange between adenosine triphosphate and creatine phosphate was studied. The substrate concentrations are in the 1–10 mM range, the linewidths and chemical shift differences are 50 Hz and 300 Hz, respectively, and data acquisition time for a single value of τ_{mix} was about 2 hr. It should be noted that the procedure of Bodenhausen and Ernst (9) may significantly reduce the total amount of time required to acquire the 2D FTNMR rate data.

The original rapid-quench studies on the phosphoglucose isomerase reaction suggested that the enzyme acted exclusively on the α form of Glc-6-*P* and Fru-6-*P* (12). Later studies (10, 13) using a high enzyme concentration showed that the enzyme catalyzes the isomerization of both the α and β forms of both Glc-6-*P* and Fru-6-*P*, but with a clear preference for the α forms of both isomers. The data acquired by 2D FTNMR are obtained in the steady state and thus are difficult to compare with rapid-quench experiments. The present 2D FTNMR experiments did not indicate any direct interconversion between βGlc-6-*P* and Fru-6-*P*. However, the rate constants for formation of Fru-6-*P* from αGlc-6-*P* and βGlc-6-*P* derived from rapid-quench experiments differ by at least a factor of 10 (10). Evidently, the direct interconversion between βGlc-6-*P* and Fru-6-*P* may proceed too slowly to measure in the steady state at the enzyme concentrations employed in our studies. Although the initial conversion of βGlc-6-*P* and Fru-6-*P* is very slow, a measurable quantity of Fru-6-*P* is formed from βGlc-6-*P* after an induction period as shown by the cross-peak behavior. A possible interpretation that is consistent with the model presented in Fig. 7 and the measured rate constants is that the majority of βGlc-6-*P* converted to Fru-6-*P* is anomerized to αGlc-6-*P* before the isomerization reaction.

In summary, these data demonstrate that 2D FTNMR is capable of determining the rate constants and reaction pathways involved in complex enzyme-catalyzed reactions. The nature of the 2D experiment provides several technical and interpretive advantages that should be useful in further studies of enzymatic processes *in vitro* as well as *in vivo*.

1. Hammes, G. G., ed. (1974) *Investigation of Rates and Mechanisms of Reactions* (Wiley, New York), Part 2.
2. Jackman, L. M. & Cotton, F. A. (1975) *Dynamic NMR Spectroscopy* (Academic, New York).
3. Gutowsky, H. S. & Saika, A. (1953) *J. Chem. Phys.* **21**, 1688–1694.
4. Gupta, R. K. & Redfield, A. G. (1970) *Science* **169**, 1204–1205.
5. Brown, T. R. & Ogawa, S. (1977) *Proc. Natl. Acad. Sci. USA* **74**, 3627–3631.
6. Forsén, S. & Hoffman, R. A. (1963) *J. Chem. Phys.* **39**, 2892–2901.
7. Jeener, J., Meier, B. H., Bachmann, P. & Ernst, R. R. (1979) *J. Chem. Phys.* **71**, 4546–4553.
8. Meier, B. H. & Ernst, R. R. (1979) *J. Am. Chem. Soc.* **101**, 6441–6446.
9. Bodenhausen, G. & Ernst, R. R. (1982) *J. Am. Chem. Soc.* **104**, 1304–1309.
10. Schray, K. J., Benkovic, S. J., Benkovic, P. A. & Rose, I. A. (1973) *J. Biol. Chem.* **248**, 2219–2224.
11. Bailey, J. M., Fishman, P. H. & Pentcher, P. G. (1968) *J. Biol. Chem.* **243**, 4827–4831.
12. Salas, M., Vinuela, E. & Sols, A. (1965) *J. Biol. Chem.* **240**, 561–566.
13. Plesser, T., Worster, B. & Hess, B. (1979) *Eur. J. Biochem.* **98**, 93–98.